Available online at www.sciencedirect.com
ScienceDirect
Journal of Power Sources 164 (2007) 880–884
JOURNAL OF POWER SOURCES
www.elsevier.com/locate/jpowsour

Short communication

Nanosized silicon-based composite derived by in situ mechanochemical reduction for lithium ion batteries

Xuelin Yang, Zhaoyin Wen*, Xiaoxiong Xu, Bin Lin, Shahua Huang

Shanghai Institute of Ceramics, Chinese Academy of Sciences, Graduate School, Chinese Academy of Sciences, 1295 Ding xi Road, Shanghai 200050, PR China

Received 15 May 2006; received in revised form 31 October 2006; accepted 1 November 2006
Available online 13 December 2006

Abstract

Composite consisting of nanosized silicon, Li_4SiO_4 and other lithium-rich components was synthesized using high energy mechanical milling (HEMM) method. The reactive milling of SiO with lithium metal resulted in the oxidation of lithium and silicon, and reduction of SiO. X-ray diffraction (XRD) and high-resolution transmission electron microscope (HRTEM) were used to determine the phases present in the composite. In addition, cyclic voltammetry (CV), along with constant current discharge/charge tests, was used to characterize the electrochemical properties of the resultant material. Compared with pure SiO and pure silicon as anode materials, the as-prepared composite demonstrated larger capacity and superior cyclability even at high C-rate.

Keywords: HEMM; Reduction; Silicon-based composite; Anode; Lithium ion batteries

1. Introduction

There is considerable interest in finding alternative materials with higher first efficiency, higher specific capacity, better cycling behavior and lower cost for lithium ion batteries. A vast amount of work has been devoted to replace the currently used graphite as new anode materials that form alloys with lithium [1–3]. Silicon is of special interest because of its potentially largest theoretic capacity of 4008 mA h g^{-1} for the $Li_{22}Si_4$ alloy [4]. The application of silicon anode, however, has been hindered by rapid capacity fading upon charge/discharge cycling. The capacity loss was certified mainly due to expansion/contraction of the material during the insertion/extraction of Li^+. The Fuji photo film in 1997 announced the potential use of convertible oxides containing tin and attracted remarkable attention to the possibility of alternatives [5], and afterwards a variety of different materials such as SiO_x [6], SnO–SiO mixtures [7] and metal–metalloid alloys [8] has been intensively investigated. In the case of SiO, the oxide is irreversibly reduced during the first lithiation process, resulting in the formation of nanosized clusters of amorphous silicon surrounded by Li_2O matrix. After the initial irreversible reaction, lithium reversibly reacts with this amorphous silicon. Although a total of 3 mol lithium was found to react per mol of SiO during the initial lithiation, the capacity became close to 1 mol of lithium per mol of SiO in the first delithiation cycle as well as subsequent lithiation cycles [9]. The first coulombic efficiency, therefore, was just one third and accordingly utilization ratio of cathode materials was also sacrificed. It is believed that reduction of metal oxides by high energy mechanical milling (HEMM) method is an ideal way to prepare silicon/oxide matrix composite with lower first irreversible capacity loss [10]. There is no doubt that lithium metal is the most suitable reductant for this reduction reaction, owing to its relative light mass and high reactivity towards oxide. However, direct milling of the reactants containing lithium metal led the formation of clumps of the powder owing to the melting of lithium metal (mp 180.1 °C). It is the formation of the clumps that hindered the mechanochemical reaction to further, in addition, the as-milled product also need further treatment such as grinding and sieving for the preparation of electrode film. Thus, in the research of oxide reduction by mechanochemical method, much attention has been directed to high melting-point melt (such as aluminum [10]) as reductant at the expense of part of reversible capacity,

* Corresponding author. Tel.: +86 21 52411704; fax: +86 21 52413903.
E-mail address: zywen@mail.sic.ac.cn (Z. Wen).

0378-7753/$ – see front matter © 2006 Elsevier B.V. All rights reserved.
doi:10.1016/j.jpowsour.2006.11.010

and moreover, lithium-containing component (such as Li_2O_2) was also needed for the improvement of cycling performances.

Here we report, for the first time to our knowledge, a reversible capacity (varying from 540 to 760 mA h g^{-1} at different C-rate) from a nanosized silicon-based composite, prepared by in situ mechanochemical reduction using SiO and lithium metal as starting materials. The advantages of this kind of composite as anode were: (1) in situ formation of nanosized silicon (<10 nm) instead of commercial nanosized silicon with high preparation cost as the insertion/extraction host of Li^+; (2) highly distribution of nanosized silicon particles during the milling step, further dispersion process for nanosized powders could be avoided; (3) effective buffering of volume changes owing to the existence of lithium-rich component matrix; and (4) high reversible capacity with greatly improved first coulombic efficiency compared with SiO electrode.

2. Experimental

Silicon monoxide (SiO, 99.99%, Shanghai Chemical Co. Ltd, China) and lithium metal with a mole ratio of 5:6 were transferred to a steel vial inside an argon-filled glove box (VAC) for mechanical milling (475 rpm). The mass ratio of milling balls to reactants was 10:1. After 10 h of milling, 10 wt.% of graphite was added into the vial and further milled for 5 h. The as-milled powder was heated at 500 °C under vacuum for 5 h, and the final product was therefore obtained without any grinding and sieving. The sample was characterized by X-ray diffraction (XRD, Rigaku RINT-2000) with Cu Kα radiation and high-resolution transmission electron microscope (HRTEM, JEM-2010) to identify the phases formed.

The working electrodes were prepared by mixing the electroactive material with PVdF as binder and acetylene black as electronic conductor in the weight ratio of 85:10:5 in *N*-methyl pyrrolidinone (NMP) solvent. The slurry of the mixture was coated on a copper foil (18 μm in thickness) using an automatic film-coating equipment. The resulting film was cut into pieces with a diameter of 14 mm, pressed under 6 MPa and dried under vacuum for 12 h at 120 °C, and then assembled as working electrode in 2025 coin cells using Celgard 2400 as the separator and lithium foil as counter and reference electrodes. A solution of 1 mol L^{-1} $LiPF_6$ in EC:DMC (1:1 in weight, Guotai-Huarong New Chemical Materials Co. Ltd, China.) was employed as the electrolyte. The assembly of cells was processed in an argon-filled glove box (VAC) with oxygen and water contents less than 1 ppm. The cells were galvanostatically discharged and charged in the range of 0.02–1.5 V at different C-rate. Cyclic voltammetry (CV) was performed on a Solartron 1287 potentiostat.

3. Results and discussion

3.1. Phase analysis

X-ray diffraction patterns of pure SiO and composite powders milled for different periods were shown in Fig. 1. A weak broad peak (Fig. 1a) in the 2θ range of 10–40° indicated the amorphous feature of SiO. After 10 h of milling, the diffraction peaks of elemental silicon was observed while the broad peak of SiO vanished (Fig. 2b), implying successful reduction of SiO into elemental silicon. Intensity of (0 0 2) peak corresponding to graphite in Fig. 1c reduced drastically (Fig. 1d) after the heat-treatment whereas diffraction peaks of silicon increased significantly, indicating that the layer structure of graphite was partially destroyed. The intensity increase implied further growth of silicon particle size under heat-treatment and it was well consistent with the results estimated by Scherrer's equation. Because heat-treatment itself was helpful to the graphitization, the destroyed layer structure should be related to the reactions between graphite and residual lithium metal. Further-

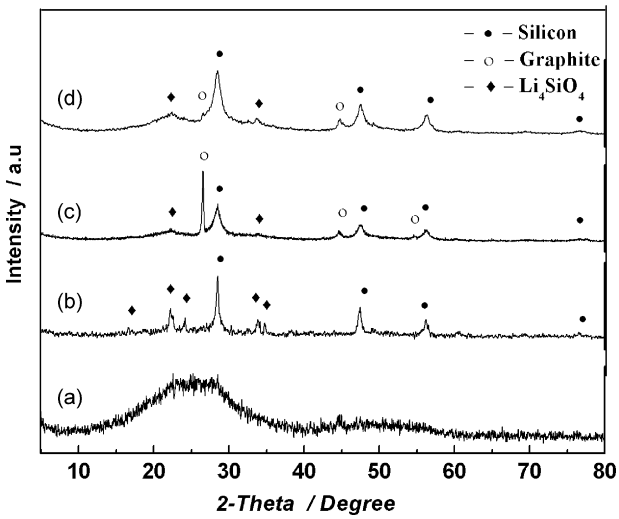

Fig. 1. X-ray diffraction patterns of (a) pure SiO; (b) mixture of SiO and lithium metal milled for 10 h; (c) the mixture of (b) further milled for 5 h with graphite additive; and (d) heat-treated at 500 °C for 5 h under vacuum.

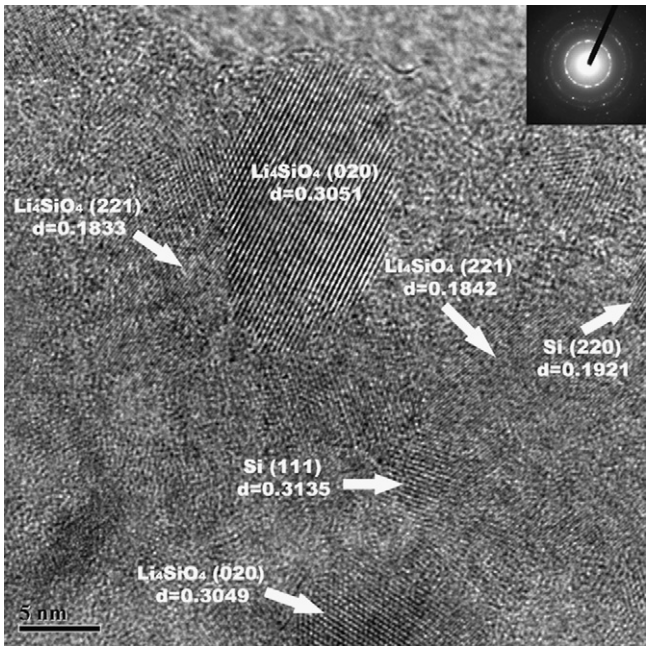

Fig. 2. HRTEM image of the composite powder after milling SiO and lithium metal for 10 h. The inset of the figure showed clear lattice fringes of Li_4SiO_4.

more, the appearance of several diffraction peaks from Fig. 1b to d confirmed the formation of lithium orthosilicate (Li_4SiO_4), which should be another main product of the mechanochemical reaction. Therefore, we presumed the reaction occurred as follows:

$$5SiO + 6Li = Li_2O + Li_4SiO_4 + 4Si$$

The inexistence of diffraction peaks corresponding to Li_2O can be ascribed to its possible amorphous structure. The above reaction could occur spontaneously during HEMM at room temperature due to the highly negative free energy change ($\Delta G^{o}_{298.15} = -2.129 \times 10^3$ kJ/mol).

Fig. 2 showed the high-resolution transmission electron microscope (HRTEM) image of the as-milled powder sample as same as in Fig. 1b. It was clear that the nanosized silicon particles dispersed in the matrix consisted of ultrafine Li_4SiO_4 grains with a few nanometers in size and some other amorphous components. The lattice fringes of selected area electron diffraction (SAED) in the inset of Fig. 2 also confirmed the presence of monoclinic Li_4SiO_4.

3.2. Electrochemical performance

Fig. 3 compared the cyclic voltammograms of the composite and pure SiO electrodes at a scanning rate of 0.05 mV s^{-1} in the potential range from 0 to 1.5 V (versus Li^+/Li). For pure SiO electrode, it experienced a sharp reduction peak below 0.2 V and a broad oxidation peak between 0.2 and 0.7 V in the first cycle. The great area difference of these two curves included in Fig. 3a demonstrated a large irreversible capacity, which should be mainly attributed to the irreversible reduction reaction from SiO to elemental silicon in the first insertion process. Furthermore, it is noted that the current and hence the charge transferred during the redox reactions decreased with cycling increased, which indicated a slow degradation process occurred in each cycle. The degradation process was related to poor electrochemical/mechanical stability of the newly formed Si/Li_2O structure. As showed in Fig. 3b, there were two broad peaks can be seen in the range of 0.6–0.9 and 0.2–0.6 V in the first reduction scan for composite electrode. The former was attributed to the formation of solid electrolyte interface (SEI) [11] film on the surface of active particles, and the latter corresponded to the presence of $Li_{12}Si_7$ according to the room-temperature equilibrium emf data [12]. Below 0.2 V, a sharp reduction peak for the insertion of Li^+ into silicon could be observed and accordingly the extraction process occurred at 0.2–0.9 V with a broad shoulder. In the subsequent cycles, a new reduction peak at 0.2 V and two oxidation peaks at 0.35 and 0.5 V, respectively, were observed. All these redox peaks were well consistent with our previous report on the cycling behavior of silicon in carbon matrix [13]. Moreover, it was interesting to find that the current of the redox reactions increased with cycling, implying that the in situ formed silicon could act as insertion/extraction host and the electrochemical reaction could take place with insertion/extraction depth increasing as a result of improved structural stability.

The specific capacity of pure SiO and composite electrodes were measured by constant current discharge/charge testing in the range 0.02–1.5 V (versus Li^+/Li) at 0.1 mA cm^{-2} and the discharge/charge profiles were shown in Fig. 4. The first discharge capacity of SiO was as high as 1816 mA h g^{-1}, but less than one third of it could be reversibly extracted. Most of this irreversible capacity was related to the reduction of SiO and part of it was used to form a SEI film on the surface of the electrode. After 10 cycles, the reversible capacity dropped to below 300 mA h g^{-1}. This indicated that the nanosized clusters of silicon in Li_2O matrix formed in the first insertion process became electrochemically inactive during repeated cycling because of poor charge-transferring environment and poor cohesion between silicon and Li_2O. In the case of composite electrode, the first discharge capacity was just 951 mA h g^{-1}, but the initial coulombic efficiency was as high as 81% because chemical reduction of SiO was avoided. After the first cycle, charge capacity was gradually improved to 798 mA h g^{-1} with the coulombic efficiency of 98% until the 10th cycle. This improvement, as similar as the increase of peak current in Fig. 3b, resulted from gradual electrolyte penetration into the inside of the electrode [6]. The voltage curves, especially after the first discharge process,

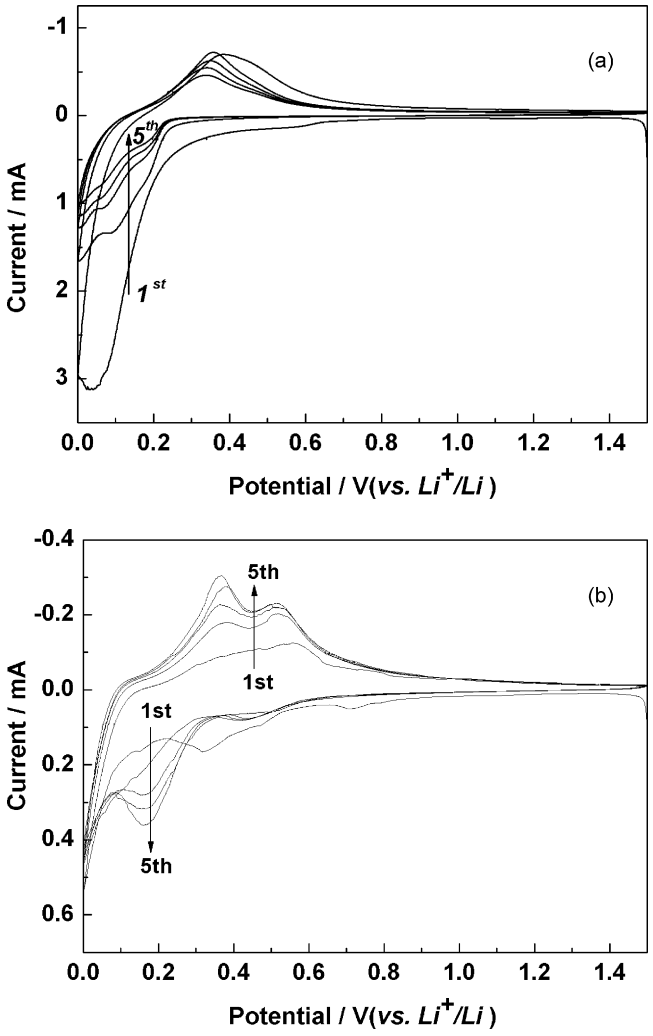

Fig. 3. Cyclic voltammograms of (a) pure SiO and (b) the as-prepared composite electrodes in a potential window from 0 to 1.5 V (vs. Li^+/Li) at the scan rate of 0.05 mV s^{-1}.

Table 1
Summarization of cycling performance for the nanosized silicon-based composite at different C-rate

	0.1C	0.2C	0.4C	0.5C	1.0C
The first charge capacity (mA h g^{-1})	770.4	731.7	632.5	616.2	356.7
The 50th charge capacity (mA h g^{-1})	762.0	690.3	592.9	544.0	615.5
Capacity change ratio (%)[a]	−0.02	−0.11	−0.13	−0.23	+1.45

[a] Relative capacity change ratio compared to the first charge capacity.

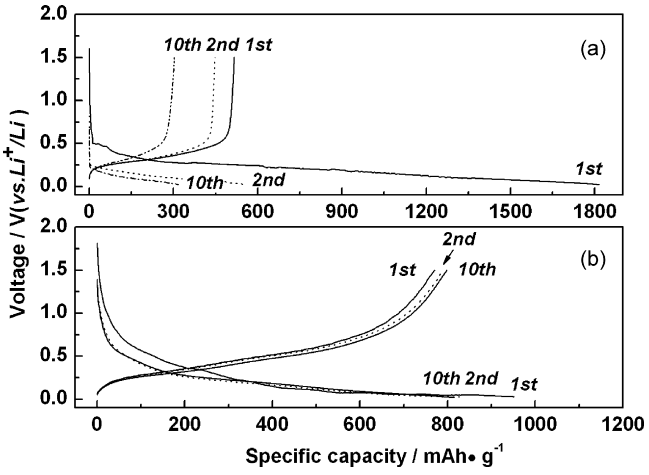

Fig. 4. Discharge and charge profiles of (a) pure SiO and (b) the composite electrodes at a constant current density of 0.1 mA cm^{-2} at different cycles.

became almost overlapping, indicating that the conductive network between silicon and the matrix was well kept and there was no obvious increase in internal resistance.

Fig. 5 exhibited cycling performance of the composite electrodes at different rates. The rate capability at 0.1C, 0.2C, 0.4C and 0.5C showed similar trend, i.e., the charge capacities gradually increased during the first 10 cycles, then remained relatively constant between the 10th and about the 30th cycle, and decreased slowly after the 30th cycle. Although the reversible capacity decreased with the increase in discharge/charge rate, the composite electrodes could exhibit stable reversible capacity at all rates. It is interesting to notice that the composite electrode

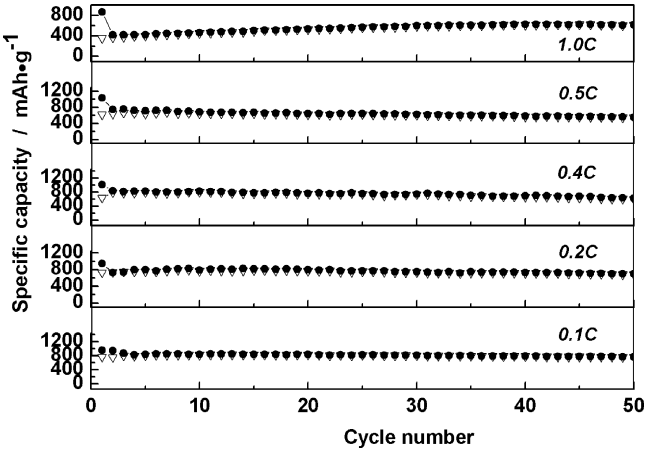

Fig. 5. C-rate capability for the discharge/charge process for the composite electrodes. Open symbols refer to charge capacity and filled symbols to discharge capacity.

just delivered a first charge capacity less than 400 mA h g^{-1} at 1C, but the increasing trend of reversible capacity could be extended to the 50th cycle. Table 1 summarized the cycling performances of the composite electrodes. As seen, the charge capacity after 50 cycles at 0.1C, i.e., 762.0 m A h g^{-1}, remained 98.9% of the first charge capacity with only 0.02% of capacity loss ratio per cycle. The capacity retention decreased gradually with increase in rate, for example, 88% of the first charge capacity was obtained (0.23% of capacity loss ratio per cycle) at 0.5C. However, charge capacity at 1C increased from 356.7 to 615.5 mA h g^{-1} (1.45% of capacity increase ratio per cycle) after 50 cycles, indicating that Li^+ was not inserted into the inside of active particles in the initial cycles, but the insertion-depth could be improved in the subsequent cycles. Furthermore, the rapid capacity fade was not observed even at high C-rate, which suggested that the electrodes could maintain their integrity over many discharge/charge cycles. The obviously improved cycling performances of the composite could be ascribed to several factors. First, nanosized silicon particles derived by mechanochemical reaction alleviated the volume change effectively. Second, the as-prepared product exhibited characteristics of a homogeneous composite in which no aggregate of nanosized silicon was observed (as shown in Fig. 3). Third, the existence of Li_4SiO_4 and other lithium-containing phases was favorable to the Li^+ transport as well as to the buffering of volume changes.

4. Conclusions

In summary, nanosized silicon-based composite powders have been firstly prepared by in situ mechanochemical reduction using SiO and lithium metal as starting materials. To the best of our knowledge, there have been no reports to date on the mechanochemical reaction used for the preparation of anode materials. The initial charge capacity of the composite electrode reached 770.4 mA h g^{-1} with coulombic efficiency of 81%. After 50 cycles, the composite electrode remained 762.0 mA h g^{-1} with only 0.02% of capacity loss ratio per cycle. It also showed excellent rate capability with a 1C-rate capacity of up to 615.5 mA h g^{-1}. The superior properties were attributed to the uniform distribution of nanosized silicon particles and the effective buffering by the lithium-rich components during discharge/charge cycling.

Acknowledgments

This work was financially supported by projects of Natural Science Foundation of China (NSFC) No. 20333040 and 50672114.

References

[1] M. Winter, J.O. Besenhard, M.E. Spahr, P. Novak, Adv. Mater. 10 (1998) 725.
[2] J. Wang, P. King, R.A. Huggins, Solid State Ionics 20 (1986) 185.
[3] T.D. Hatchard, J.R. Dahn, J. Electrochem. Soc. 152 (2005) A1445.
[4] A. Netz, R.A. Huggins, W. Weppner, J. Power Sources 1 (2003) 5271.
[5] Y. Idota, T. Kubota, A. Matsufuji, Y. Maekawa, T. Miyasaka, Science 276 (1997) 1395.
[6] J. Yang, Y. Takeda, N. Imanishi, C. Capiglia, J.Y. Xie, O. Yamamoto, Solid State Ionics 152–153 (2002) 125.
[7] H. Morimoto, M. Tatsumisago, T. Minami, Electrochem. Solid-State Lett. 4 (2001) A16.
[8] A. Netz, R.A. Huggins, W. Weppner, J. Power Sources 119–121 (2003) 95.
[9] A. Netz, R.A. Huggins, Solid State Ionics 175 (2004) 215.
[10] H.Y. Lee, S.M. Lee, Electrochem. Commun. 6 (2004) 465.
[11] Y. Liu, K. Hanai, J. Yang, N. Imanishi, A. Hirano, Y. Takeda, Electrochem. Solid-State Lett. 7 (2005) A369.
[12] W.J. Weydanz, M. Wohlfahrt-Mehrens, R.A. Huggins, J. Power Sources 81–82 (1999) 237.
[13] X.L. Yang, Z.Y. Wen, X.J. Zhu, S.H. Huang, Electrochem. Solid-State Lett. 8 (2005) A481.